Journal of Metals, Materials and Minerals, Vol.21 No.1 pp.1-8, 2011

Chevron Crack Initiation in Multi-Pass Drawing of Inclusion Copper Shaped-Wire

Somchai NORASETHASOPON

Department of Mechanical Engineering, Faculty of Engineering,
King Mongkut's Institute of Technology Ladkrabang, Chalong-krung Road,
Ladkrabang, Bangkok 10520, Thailand

Abstract

In the copper superfine wire drawing, the internal cracks such as chevron cracks and breakage of the wire were fatal to the success of quantitative drawing operations. This paper shows how the main process parameters, the drawing pass numbers, influence the plastic deformation, hydrostatic stress, maximum principal tensile stress and chevron cracks initiation investigated by FEM simulation. The effect of the lateral and longitudinal sizes of a central cylindrical inclusion in the multi-pass copper shaped-wire drawing was studied. The plastic deformation, plastic strain, hydrostatic stress and maximum principal tensile stress of the copper shaped-wire containing an inclusion were obtained from simulation results. A ductile fracture criterion was chosen from literature, a large number of ductile fracture initiation criteria, to predict the chevron crack initiation of the drawn copper shaped-wire for this investigation. The problem of chevron cracks initiation for the investigated material was solved. This investigation provided very good results.

Key words: Copper shaped-wire, Cracks initiation, Chevron cracks, Ductile fracture criterion

Introduction

Nowadays, various superfine wires are widely used in commercial products such as a fishing line, screw, pin, bolt, steel cord, sawing wire, cable, spring, screen mesh, mesh of filter, wire rope, stiffening wire, antenna, sensor, bonding wire, electronic wire, etc. Superfine steel wires are used for printing meshes, filters, steel cords, saw wires, wire ropes, precision springs, precision screws and precision pins. Superfine non-ferrous wires are used for ultra small motors, semiconductor bonding wires, magnet wires, materials for electronic components, and electrode wires for electrical-discharge processing as shown in Figure 1. Multiple research efforts have been made to develop ultra small motors in Japan. To further improve the performance and the efficiency of such motors, a cross-section of the magnet wire for the motor needs to be changed from circular to square as shown in Figure 2. At present, the size of this shaped (square) wire is suggested to be in a range of 300 to 500 micrometers [(1)].

Superfine wire processing requires a large number of drawing-passes and intermediate softening heat treatments. In some cases, internal or chevron cracks and breakage of wires occur. This results in high manufacturing cost. In particular, for wire with diameters of 0.1 mm or less, the product price increases exponentially with the decrease of the wire diameter [(2)]. Raskin [(3)] reported the causes of wire breakage while copper wire drawing, and based his report on a survey of 673 wire breaks. The report concludes that 52%, 13%, 13%, 5%, 5%, and 12% are attributable to inclusion, central bursting or cupping, tension break, weld break, silver break and others, respectively, as shown in Figure 3. It can obviously be observed that the most important problem of wire breakage while copper wires drawing is wire breakage due to inclusions (WC or sintered hard alloy). Figure 4 shows the wires fracture due to an inclusion while copper wire drawing.

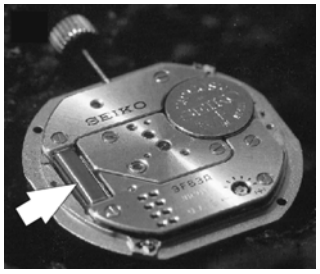

Figure 1. Use of the superfine wires in the fields of precision equipment and semiconductor: magnet wire for wristwatch (courtesy of SEIKO Corp.).

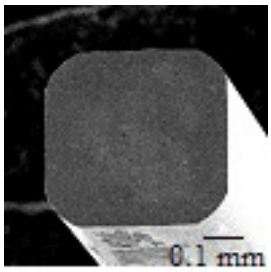

Figure 2. The drawn copper (99.99 wt%) shaped-wire.

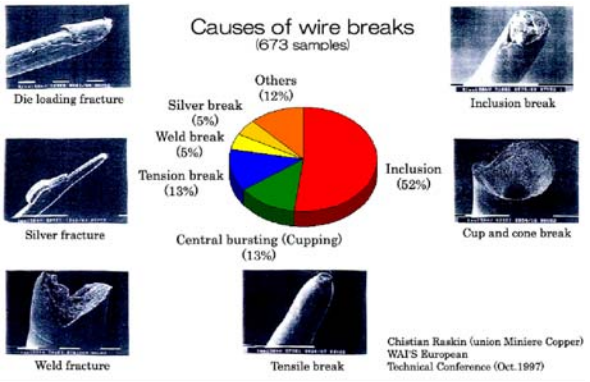

Figure 3. Causes of wire breakage while copper wire drawing [3].

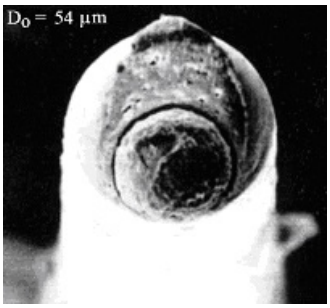

Figure 4. Wire breakage due to an inclusion.

The inclusion/metal system may be simplistically considered as a composite material with the inclusions acting as the aggregate and the metal as the matrix [4-9]. It is apparent that there are a number of factors that affect the performance of the whole. Among these are the volume percentage, shape, orientation, and mechanical properties of the inclusions and the direction of the principal stresses with respect to this orientation. The failure of the inclusion wire during drawing can be attributed to ductile fracture that initiates after necking begins. Ductile fracture in wire matrix is a multi-step mode of material failure that is known to be the void initiation, growth and coalescence [10]. The coalescence of the voids forms a continuous fracture surface followed by failure of the remaining annulus of the wire matrix usually on plane at 45° to the drawing direction. Voids can initiate at inclusions or secondary phase particles by de-cohesion of the particle-matrix interface or fracture of the particle in the center of the neck region. The internal or chevron cracks as shown in Figure 5 are typical ductile fractures due to plastic deformation in wire drawing. Figure 6 shows the chevron cracks that occur along the non-inclusion wire centerline on the longitudinal cross section of a copper wire. While the inclusion was passing through the reduction zone of the die, the highest tensile stress, the tensile stress at the inclusion-leading-edge strongly influenced this plastic deformation [11-14]. This crack initiation will occur if the tensile strain-energy density reaches a critical value which can be described by a ductile fracture criterion that was proposed by Cockcroft and Latham [15].

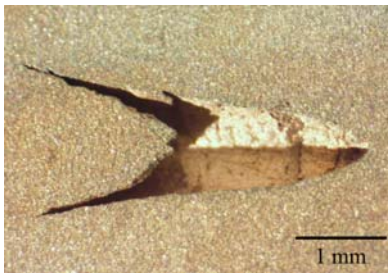

Figure 5. Chevron cracks at the centerline of the copper wire.

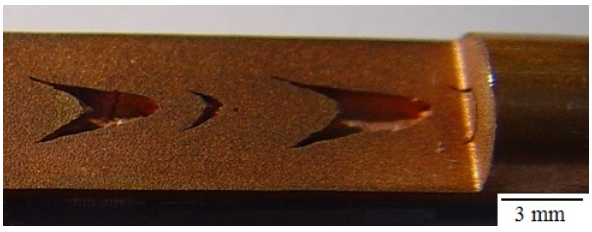

Figure 6. Chevron cracks on the longitudinal cross section of a copper wire.

The wire breakage, defect and chevron cracks are fatal to industrial scale high-purity copper superfine wire production [2-12]. To reduce these unsatisfactory situations and thus increase production quantity, the appropriate process parameters and high-purity material should be selected and used in copper superfine wire drawing [2-14]. The objective of this investigation was to determine how the main process parameters, the drawing pass numbers, influence the plastic deformation, hydrostatic stress, maximum principal tensile stress and internal or chevron cracks initiation occurring by FEM simulation.

Basic Theory

Wire Drawing

The wire drawing process is classified as an indirect compression process, in which the major forming stress results from the compressive stress as a result of the direct tensile stress exerted in the drawing. A converging die surface in the form of a truncated cone is used. Analytical or mathematical solutions [16] are obtained by a free body equilibrium method. By summing up the forces in the wire drawing direction of a free body equilibrium diagram at an element in the reduction zone, the longitudinal stress is obtained. By summing up the forces in the radial direction, the radial or die-breaking stress is obtained. Then combining those results, integrating the resulting differential equation, and simplifying, the equation for the average drawing stress is obtained as shown in equation (1).

$$\frac{\sigma_x}{\bar{\sigma}} = \frac{1+B}{B}\left[1-\left(\frac{D_f}{D_o}\right)^{2B}\right] \tag{1}$$

Where D_o and D_f are the original and final diameters, respectively, and B is equal to $\mu \cot \alpha$

The same approach can be used to yield equations of essentially the same form for such similar operations as drawing of a wide strip through a wedge-shaped die. In the case of the drawing of a strip through a wedge-shaped die in plane-strain, the following equation (1) is obtained:

$$\frac{\sigma_x}{S} = \frac{1+B}{B}\left[1-\left(\frac{h_f}{h_o}\right)^{B}\right] \tag{2}$$

where S is the yield stress ($2\sigma_o/\sqrt{3}$) in a plane-strain compression test according to the von Mises criterion, σ_o is the yield stress in uniaxial tension, h_o is the initial thickness and h_f is the final thickness.

Ductile Fracture Criteria

The plastic work criterion is based on the assumption that the material can only absorb a certain amount of energy. This energy criterion was proposed in this form by Freudenthal [17]. The Rice & Tracey criterion is based on a theoretical study of the growth of a void in an infinite rigid, perfect plastic matrix. The Oyane criterion is derived from a plasticity theory for porous materials, assuming that the volumetric strain has a critical level. The Cockroft & Latham [15] criterion considers the effect of the maximum principal stress over the plastic strain path.

Cockcroft and Latham have proposed that a criterion [15] for the fracture of a ductile material in tension is that in which the tensile strain energy reaches a critical value for a given condition of loading as follows [16]:

$$\int_0^{\varepsilon_f} \sigma^* \, d\bar{\varepsilon} \;=\; C \tag{3}$$

where $\bar{\varepsilon}$ is equivalent strain, ε_f is fracture strain, σ^* is maximum principal tensile stress attained in the specimen under axial loading, and C is constant for a material at a given temperature and strain rate as determined from an uniaxial tension test. A material will fracture when it achieves a strain-energy density equal to the above integral. C may be determined from independent test data such as for the tensile test using Bridgman's analysis [16].

This criterion can be successfully applied to cold working processes [16, 18], such as to predict the incidence of cracking along the centerline in cold rod drawing and extrusion for a small reduction which causes chevron crack formation where tensile stresses prevail.

The goal of this research is to predict the internal or chevron cracks initiation of the drawn copper shaped-wire. A ductile fracture criterion, Cockcroft and Latham criterion, was chosen for this investigation.

Finite Element Analysis

The finite element method is a powerful tool for the numerical solution of wire drawing. With the advance in computer technology, wire drawing can be modeled with relative ease. In this, FEM have the following six steps. In the first step, Shape Functions, the finite element method, expresses the unknown field in terms of the nodal point unknown by using the shape functions over the domain of the element. In the second step, Material Loop, the finite element method, expresses the dependent flux fields such as the strain or stress in terms of the nodal point unknowns. In the third step, Element Matrices, the finite element method, equilibrates each element with its environment. In the fourth step, Assembly, the finite element method,

assembles all elements to form a complete structure in such a manner as to equilibrate the structure with its environment. In the fifth step, Solving Equations, the finite element method, specifies the boundary conditions, namely, the nodal point values on the boundary, and the system equations are partitioned. In the sixth step, Recover, the finite element method, recovers the stresses by substituting the unknown nodal values found in the fifth step back into the second step to find the dependent flux fields such as strain, stress, etc.

A two-dimensional finite element method was used for analyzing the effects of a central and non-central inclusion on stresses, strains and plastic deformation in copper shaped-wire drawing. Figure 7 shows the analytical model used. The black part was an inclusion in a copper shaped-wire. The authors assumed that the inclusion was a sintered hard alloy (WC). Table 1 shows the material properties and the drawing conditions that were used in this analysis.

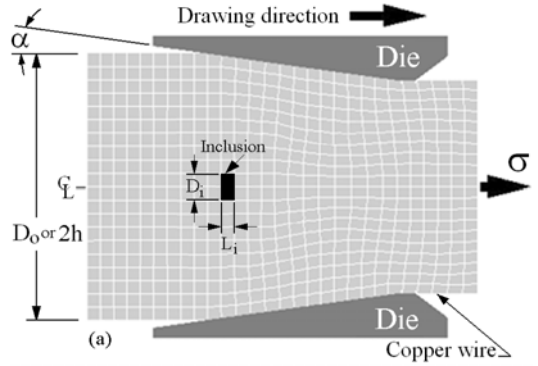

Figure 7. 2-D FEM model used in this copper shaped-wire drawing simulation.

Table 1. Material properties and drawing conditions used for FEA.

	Copper (wire)	WC (inclusion)
Young's modulus, E (MPa)	120000	1000000
Yield stress, σ_Y (MPa)	150	1000
Poisson's ratio, ν	0.3	0.22
Die half-angle, α (°)	8	
Reduction, Re (%)	17.4, 20	
Coefficient of friction, μ	0.05	

The model solution was obtained by using the MSC.MARC program. The element type, wire and inclusion material, die material, friction model and analysis type were set as quadrilateral, isotropic (elastic-plastic), rigid, Coulomb and plane strain (large deformation), respectively. The authors assumed that the wire and the inclusion matrix were joined at the boundary during the process. In this analysis, the wire was considered to be a copper shaped-wire with a hard inclusion subjected to steady deformation. It is also assumed that the inclusion can completely transfer the axial tensile stresses. The longitudinal inclusion size ratio (L_i/D_o) equal to 0.05, 0.1, 0.2, 0.3 and 0.4 was used. The lateral inclusion size ratio (D_i/D_0) equal to 0.1, 0.2, 0.3, and 0.4 was also used. The die half-angle (α), reduction per pass (R/P) and coefficient of friction (μ) were set at 8 degrees, 20 %, and 0.05, respectively.

Results and Discussion

Stresses, Strains and Plastic Deformation Behaviour

The stresses, strains and plastic deformation behaviour of the copper shaped-wire that contained a central inclusion for D_i/D_o equal to 0.1 and 0.3 where L_i/D_o was equal to 0.05 during five passes of drawing were obtained by FEM simulation. Figure 8 shows the distribution of hydrostatic stress and plastic deformation of the copper shaped-wires containing a central inclusion during multi-pass drawing for D_i/D_o = 0.1 and 0.3 and L_i/D_o = 0.05 where Re = 20% and α = 8°.

For the first pass drawing, the inclusion was slightly deformed because of its hardness, resulting in large copper deformation. The inclusion deformation occurred when copper shaped-wire was repeatedly drawn. The necking behavior and the relationship between the lateral neck size and the lateral inclusion size are the same as described in the case of the single-pass drawing of copper shaped-wire containing a central and non-central cylindrical inclusion. While drawing the wire containing a central inclusion, it was found that the hydrostatic and maximum principal tensile stresses in front of the inclusion-leading-edge increased as D_i/D_o increased.

The highest value of the hydrostatic and maximum principal tensile stresses in front of the inclusion-leading-edge occurred where the inclusion-leading-edge exited and was outside the die. When comparing between the lateral and longitudinal inclusion sizes effects, the maximum tensile stress was stronger influenced by L_i/D_o than D_i/D_o. The

wire deformation, inclusion deformation and maximum tensile stress also increased as the drawing pass numbers increased.

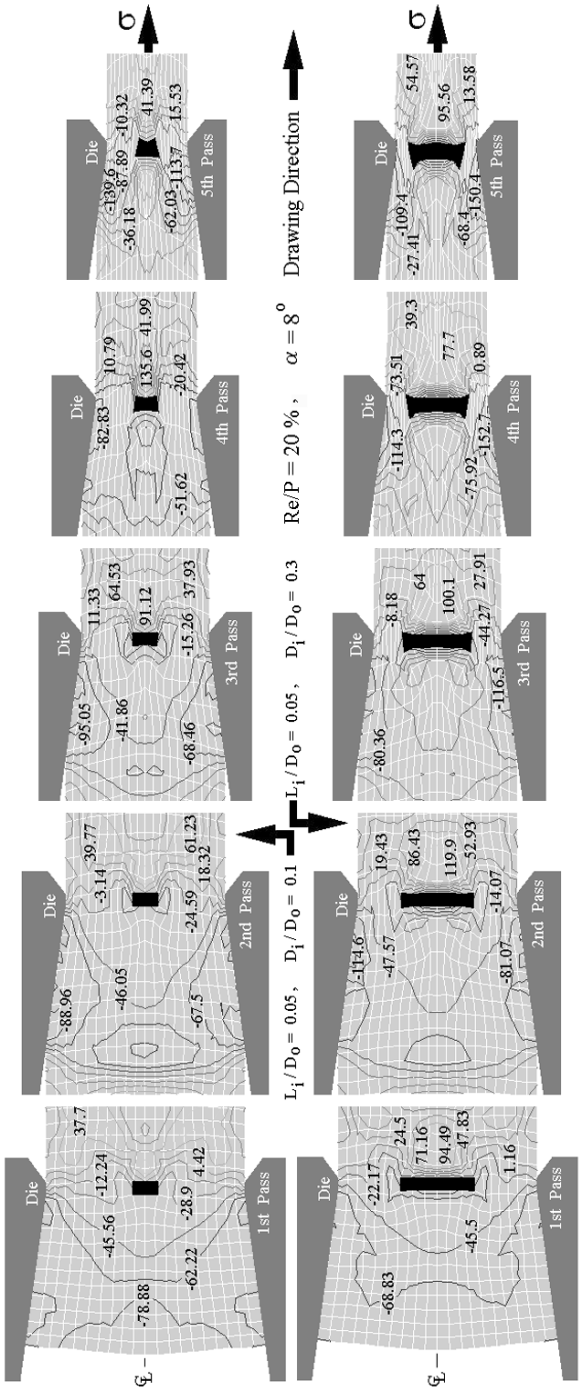

Figure 8. Distribution of hydrostatic stress and plastic deformation of the copper shaped-wires containing a central inclusion during multi-pass drawing for D_i/D_o = 0.1 and 0.3 and L_i/D_o = 0.05 where Re = 20% and α = 8°.

Internal or Chevron Cracks Initiation

The Cockcroft & Latham criterion was selected and used as the damage value to estimate if and where an internal or chevron crack will occur during the copper shaped-wire drawing. For the FEM simulation, the Cockcroft & Latham criterion can be written as follows:

$$\sum_{i=1}^{n} (\sigma^* \Delta\bar{\varepsilon})_i \quad = \quad C \tag{4}$$

where n is the number of steps in the simulation, $\Delta\bar{\varepsilon}$ is the incremental effective strain ($\Delta\bar{\varepsilon} = \bar{\varepsilon}_i - \bar{\varepsilon}_{i-1}$), σ^* is the maximum principal tensile stress in the element, and C is the material constant or the critical damage value. The critical damage value (C) of the material, copper, used in this investigation was determined to be 0.664 in the tensile test by a universal tensile testing machine at room temperature.

The results of the analysis described in section 4.1 showed that the maximum tensile stress over the entire FEM mesh in all cases of those simulations occurred in front of the inclusion-leading-edge. If the summation of equation (4), C, exceeds the critical damage value, an internal crack or chevron crack should therefore occur in front of the inclusion-leading-edge.

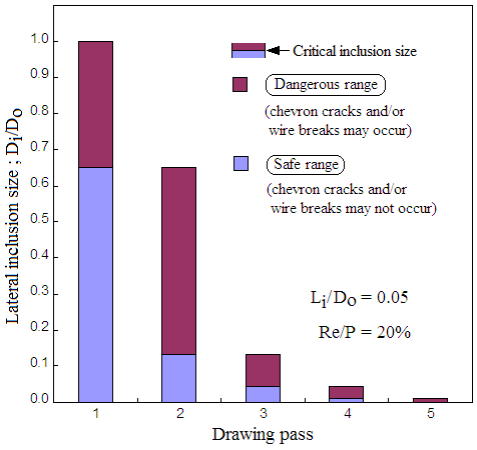

Figure 9. Influence of the lateral inclusion size and drawing pass number on chevron crack initiation in the multi-pass drawing of the copper shaped-wire containing a central cylindrical inclusion for L_i/D_o = 0.05 where Re/P = 20%.

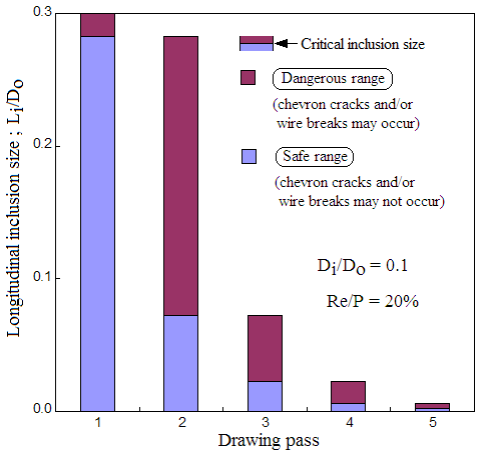

Figure 10. Influence of the longitudinal inclusion size and drawing pass number on chevron crack initiation in the multi-pass drawing of the copper shaped-wire containing a central cylindrical inclusion for D_i/D_o = 0.1 where Re/P = 20%.

The influence of the lateral and longitudinal inclusion size on the chevron crack initiation in the multi-pass drawing of the copper shaped-wire containing a central cylindrical inclusion was obtained. Figure 9 shows the critical lateral inclusion sizes, 0.648, 0.134, 0.038, 0.009 and 0.001, in the first, second, third, fourth and fifth passes, respectively, for L_i/D_o = 0.05 where Re/P = 20%. Figure 10 shows the critical longitudinal inclusion sizes, 0.283, 0.072, 0.023, 0.006 and 0.001, in the first, second, third, fourth and fifth passes, respectively, for D_i/D_o = 0.1 where Re/P = 20%.

These critical lateral and longitudinal inclusion sizes can also be plotted as a function of the total reduction of cross-sectional area as shown in Figures 11 and 12. The "inclusion size" as indicated in Figures 9 to 12, the initial inclusion size, means the size of an inclusion in an undrawn wire.

When the initial inclusion sizes (lateral and longitudinal inclusion sizes) are very small, a large number of drawing passes can be performed without chevron cracks initiation. As the results, more than five passes of the copper shaped-wire drawing can be performed without chevron cracks initiation when the initial inclusion size is less than 0.001. The number of the drawing passes that can be performed without chevron cracks initiation rapidly decreased as the initial inclusion size increased. In this case, chevron cracks initiation was found in the first pass of the copper shaped-wire drawing when the initial lateral inclusion size was equal to 0.648 for L_i/D_o = 0.05. Chevron cracks initiation was found in the first pass of the copper shaped-wire drawing when the initial longitudinal inclusion size (inclusion length) was equal to 0.283 for D_i/D_o = 0.1.

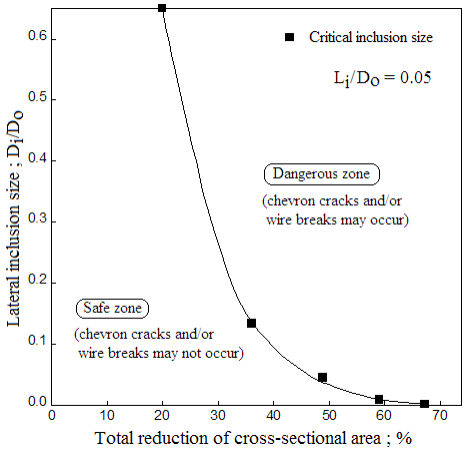

Figure 11. Influence of the lateral inclusion size and total reduction of cross-sectional area on chevron crack initiation in the multi-pass drawing of the copper shaped-wire containing a central cylindrical inclusion for L_i/D_o = 0.05 where Re/P = 20%.

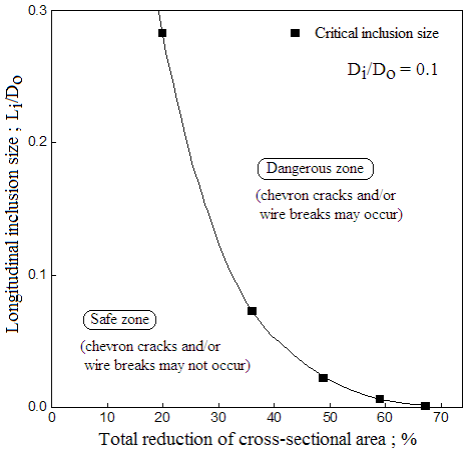

Figure 12. Influence of the longitudinal inclusion size and total reduction of cross-sectional area on chevron crack initiation in the multi-pass drawing of the copper shaped-wire containing a central cylindrical inclusion for D_i/D_o = 0.1 where Re/P = 20%.

Conclusions

1. Necking occurred on the copper shaped-wire surface in front of the inclusion-leading-edge near the inclusion boundary.

2. Inclusion deformation occurred when copper shaped-wire was repeatedly drawn. The highest value of the hydrostatic and maximum principal tensile stresses in front of the inclusion-leading-edge occurred where the inclusion-leading-edge exited and was outside the die. The drawing pass numbers strongly influenced the wire deformation, inclusion deformation and maximum principal tensile stress in multi-pass copper shaped-wire drawing.

3. A large number of drawing passes can be performed without chevron cracks initiation when the initial inclusion sizes, lateral and longitudinal inclusion sizes, were very small. This initial inclusion size inversely and strongly influenced the number of the drawing passes that can be performed without chevron cracks initiation. More than five passes of the copper shaped-wire drawing can be performed without chevron cracks initiation when the initial inclusion size is less than 0.001.

The internal or chevron cracks may occur when the inclusion size is larger than the critical inclusion size and finally, wire breaks may also occur.

Acknowledgments

The author wishes to express his appreciation to the Director of the National Metal and Materials Technology Center (MTEC), National Science and Technology Development Agency, Thailand, for his support and assistance in many details of the finite element program "MSC.MARC" for this problem simulation. The author would like to thank Ido R., and Shinohara T., Department of Precision Mechanics, School of Engineering, Tokai University, Japan, and Nissapakul, P., Tangsri, T., and Pramaphant, P., Department of Mechanical Engineering, Faculty of Engineering, King Mongkut's Institute of Technology Ladkrabang, Thailand, for giving him valuable discussion and comments.

References

1. Nikkei-Mechanical (2000). *The motor efficiency competition.* Tokyo, Nikkei: 40-44.

2. Yoshida, K. (2000). Technological trend and problem of wire drawing of various super fire wires *J. Jpn. Soc. Technol. Plast.* **41**: 194-198.

3. Raskin, C. (1997) In: *Proceedings of the WAI International Technical Conference*. Italy.

4. Amstead, B. H., Ostwald, P. F. & Begeman, M. L. (1987). Manufacturing processes. Singapore, Wiley: 1-687.

5. Johnson, H. V. (1984). Manufacturing processes. Bennett & McKnight: 14-581.

6. Kutz, M. (1998). *Mechanical engineers' handbook.* New York, NY: Wiley: 3-1205.

7. Colangelo, V. J. & Heiser, F. A. (1989). *Analysis of metallurgical failures.* Singapore: Wiley: 240-322.

8. Avitzur, B. (1968). *Metal forming: Processes and analysis*. New York, NY: McGraw-Hill: 153-258.

9. Avitzur, B. (1971). Study of flow through conical converging dies. In A. L. Hoffmanner (Ed.). *Metal forming: Interrelation between theory and practice*. New York, NY: Plenum Press: 1-46

10. Garrison Jr., W. M. & Moody, N. R. (1987). Ductile fracture. *J. Phys. Chem. Solids* **48(11)**: 1035-1074.

11. Campos, H. B. & Cetlin, P. R. (1998). The influence of die semi-angle and of the coefficient of friction on the uniform tensile elongation of drawn copper bars. *J. Mater. Process. Tech.* **80-81(1)**: 388-391.

12. De Castro, A. L. R., Campos, H. B. & Cetlin, P. R. (1996.) Influence of die semi-angle on mechanical properties of single and multiple pass drawn copper. *J. Mater. Process. Tech.* **60(1-4)**: 179-182

13. Norasethasopon, S. & Yoshida, K. (2006). Influences of inclusion shape and size in drawing of copper shaped-wire. *J. Mater. Process. Tech.* **172(3)**: 400-406

14. Norasethasopon, S. & Yoshida, K. (2006). Finite-element simulation of inclusion size effects on copper shaped-wire drawing. *Mat. Sci. Eng. A-Struct.* **422(1-2)**: 252-258.

15. Cockcroft, M. G. & Latham, D. J. (1968). Ductility and workability of metals. *J. Inst. Met.* **96**: 33-39.

16. Edward, M.M. (1991). *Metalworking science and engineering.* New York, NY: McGraw- Hill: 397-462

17. Freudenthal, A. M. (1950). *The inelastic behavior of solids.* New York, NY: Wiley.

18. Clift, S.E, Hartley, P., Sturgess, C.E.N. & Rowe, G.W. (1990). Fracture prediction in plastic deformation processes. *Int. J. Mech. Sci.* **32(1):** 1 –17.